Determination of Rate Constants by the Frequency Response Method: CO on Pt/SiO_2

A technique based upon transmission FTIR to obtain rate constants for adsorption and desorption over supported metal catalysts has been developed and tested. The technique requires the use of a sinusoidal perturbation function imposed on steady state linearized adsorption-desorption kinetics. The measurement of a phase lag between the sinusoidal inlet gas phase forcing concentration and the response of surface coverage, together with a measurement of the maximum amplitudes of the forcing function and surface response enable the calculation of the relevant adsorption and desorption rate constants.

The technique has been successfully applied to the measurement of both adsorption and desorption rate constants for CO adsorbed on a 1% Pt/SiO_2 catalyst. The values obtained for these rate constants at 343 K were: $K_a = 0.147\ s^{-1}$ and $K_d = 7.28 \times 10^{-3}\ s^{-1}$. A sticking coefficient corresponding to the adsorption of weakly bonded CO on Pt under conditions of high CO surface coverage was obtained.

Yao-En Li
David Willcox
Richard D. Gonzalez
Department of Chemical Engineering
University of Illinois
Chicago, IL 60680

Introduction

One of the pervasive problems in heterogeneous catalysis is the assessment of the rate constants and the nature of active sites participating in a reaction pathway. Partial solutions to the problem are afforded by static and dynamic chemisorption techniques that measure the total number of sites to which an adsorbate bonds, but give no information regarding rate constants and site energetics. Temperature-programed desorption measures site density as a function of binding energy and yields a convoluted rate constant. It, however, is incapable of measuring adsorption on weakly bonding sites. The technique of frequency response chemisorption offers an alternative route for the measurement of rate constants and on the nature of adsorption sites.

The frequency response technique is used widely in process control theory and has been extensively used in process identification procedures. In the area of catalysis, this method is not well known. Naphthali and Polinski (1963), for the first time, have shown the usefulness of the frequency response chemisorption method applied to a batch system. Yasuda (1976) further perfected this technique. Goodwin et al. (1985) applied the method to study the role of the support on hydrogen chemisorption over supported rhodium catalysts.

Jones et al. (1972) and Schwarz and Madix (1974) applied the frequency response method to an ultra-high vacuum study of the measurement of intrinsic desorption rate constants and reaction probabilities. (They referred to it as the modulated molecular beam technique.) Instead of changing the volume of the reactor in a sinusoidal fashion as in the frequency response method (Naphthali and Polinski, 1963), they varied the intensity of the molecular beam sinusoidally. From the phase lag of the response function, the desorption rate constant was evaluated.

In this article, we report on a method based upon transmission Fourier transform Infrared Spectroscopy, which we developed to determine the intrinsic rate constants for the adsorption and desorption of CO on a Pt/SiO_2 catalyst under actual flow conditions.

Mathematical Formulation of the Frequency Response Method in a Flow System

The method for simple flow through a packed bed microreactor can be summed up as follows. The mass balance for the *i*th species on the surface is:

$$\frac{dn_i}{dt} = K_a n_g (L - n_i)^m - K_d n_i^m \qquad (1)$$

When $m = 2$, adsorption occurs by a dissociative process, and

---

Correspondence concerning this paper should be addressed to R. D. Gonzalez.
Current address of Y. Li: American Air Liquide, Chicago Research Center, Chicago IL.

when $m = 1$, the process is nondissociative. For a mechanism involving a precursor stage, the adsorption order is $m = 1$ and for desorption, $m = 2$. In the gas phase, the mass balance is:

$$\frac{dn_g}{dt} = \frac{n^{in} - n_g}{\tau} - K_a n_g (L - n_i)^m + K_d n_i^m \tag{2}$$

Equations 1 and 2 can be nondimensionalized by using the nondimensional variables defined in the nomenclature

$$\alpha \frac{d\theta_i}{d\xi} = K_1 N (1 - \theta_i)^m - K_2 \theta_i^m \tag{3}$$

and

$$\frac{dN}{d\xi} = N^{in} - N - K_1 N (1 - \theta_i)^m + K_2 \theta_i^m \tag{4}$$

Equations 3 and 4 can be linearized by introducing a small perturbation around steady state as follows:

$$\begin{aligned} \Delta N &= N - 1 \\ \Delta N^{in} &= N^{in} - 1 = Q \sin(\omega\xi) \\ \Delta\theta &= \theta - \theta^{ss} \end{aligned} \tag{5}$$

Substituting these perturbation variables and neglecting the second-order term $\Delta N \Delta\theta$, Eqs. 3 and 4 become:

$$\alpha \frac{d\Delta\theta_i}{d\xi} = X\Delta N - Y\Delta\theta_i \tag{6}$$

$$\frac{d\Delta N}{d\zeta} = -(1 + X)\Delta N + Y\Delta\theta_i + Q \sin(\omega\zeta) \tag{7}$$

where

$$X = K_1(1 - \theta_i^{ss})^m, \qquad Y = m[K_1(1 - \theta_i^{ss})^{m-1} + K_2(\theta_i^{ss})^{m-1}] \tag{8}$$

Using the Laplace Transformation method, the response of the surface coverage with respect to the perturbation frequency can be obtained in terms of real time as follows:

$$\Delta\theta_i(\xi) = \frac{Q}{2i} G(i\omega) e^{i\omega\xi} + \frac{Q}{2i} G(-i\omega) e^{-i\omega\xi} + \sum_{j=1}^{m} C_j e^{P_j \xi} \tag{9}$$

where $G(i\omega)$ is the transfer function and P_j is the poles of the transfer function. For a stable system, the poles (P_j) must be less than zero. This means that as time approaches infinity, the last term in Eq. 9 vanishes to give

$$\Delta\theta_i(\xi) = M \sin(\omega\xi - \phi) \tag{10}$$

where

$$M = \frac{X}{\sqrt{(Y - \alpha\omega^2)^2 + (Y + \alpha + \alpha X)^2 \omega^2}} \tag{11}$$

and

$$\tan(\phi) = \frac{(Y + \alpha + \alpha X)\omega}{Y - \alpha\omega^2} \tag{12}$$

ϕ is the phase lag between the surface coverage of the adsorbate and the forcing inlet, and M is the ratio of the maximum amplitude of the response of surface coverage to the maximum amplitude of the input function. From Eqs. 11 and 12, we can see that ϕ and M are the experimentally measurable quantities, α is a parameter which is related to the catalyst property and operating conditions, and ω is the experimental variable. Hence, X and Y can be calculated.

Examination of Eq. 12 shows a discontinuity in the tan (ϕ) when $Y = \alpha\omega_c^2$. For this particular forcing frequency (ω_c), X can be calculated from the measured maximum amplitude ratio M_c using Eq. 11.

Both X and Y are related to the adsorption and desorption rate constants through Eq. 8. This means that in principle both the adsorption and desorption rate constants can be calculated through the measurement of the phase lag (ϕ), the maximum amplitude ratio (M), and the steady state surface coverage (θ^{ss}).

In general, the response of a system to a sinusoidal wave input can be divided into two periods: the transient and stable periods. The first is the transient period, which converges into a steady-state response period. Since we have assumed that the poles of the transfer function, Eq. 9, are negative, Eqs. 11 and 12 become valid under steady-state response conditions. For this reason, data must be taken after the unstable transient dies out for each forcing frequency.

Experimentally, the task to be followed is to generate two sinusoidal forcing wave functions which have the following form:

$$\begin{aligned} V_{co} &= V'_{co} + Q \sin(\omega\xi) \\ V_{He} &= V'_{He} - Q \sin(\omega\xi) \end{aligned} \tag{13}$$

such that the total flow rate stays constant:

$$F = V_{co} + V_{He} = \text{constant} \tag{14}$$

Another aspect to be taken into account in the design of the experiment is that the amplitude of the forcing function should be kept as small as possible due to the neglect of the second-order $\Delta N \Delta\theta$ term during linearization of Eqs. 3 and 4.

Experimental Study

Infrared cell reactor

In order to meet the requirements of this study, an infrared cell reactor should at least conform to the following:

1) The residence time in the infrared cell reactor should be less than the time required to scan the spectrum.

2) The reactant gases should preferably be forced through the sample disk with little or no leakage around the edges.

3) The outlet from the infrared cell reactor should be interfaced properly with a quadrupole mass spectrometer or another suitable analytical measuring device for analyzing the gas phase.

4) The cell should be constructed to handle adequate heating schedules.

Nagai et al. (1986) have recently described an infrared cell reactor which meets these requirements. Briefly, the cell dimensions are such that the net reactor-cell volume is 1.5 mL at a flow rate of 100 mL/min. With this cell, residence times of 1.0 s can be achieved. In this study, four coadded interferograms per second were used. Thus, a residence time, which was close to that required for the transient response studies, was obtained.

Flow system

A block diagram of the associated components used in the flow system is outlined in Figure 1. The reactor was placed in the sample chamber of an FTIR (FTS40, Digilab) spectrometer. The gas-phase composition in the reactor was monitored by a quadrupole mass spectrometer (QMS 112, Balzer). The infrared data were processed in a 3240-SPC data station (Digilab) and could be transferred to a personal computer (IBM-AT). The inlet gas flow rate was controlled by using Tylan (model FC260) electronic flow controllers. The sinusoidal forcing frequency was obtained by feeding two analog signals from the IBM-AT personal computer to the electronic flow controllers. These signals were adjusted to maintain a constant total flow rate as required by Eq. 14. The actual flow rates passing through the controllers were fed back to the multiplexer (HP-3421A), which was controlled by an HP computer (HP-85B). The flow controllers were calibrated by the manufacturer using gas mixtures which were close to those used in this study. The calibration was rechecked in our laboratory by means of a bubble flowmeter and a gas chromatograph. The temperature of the reactor was controlled by a temperature programmer (Valley Forge Instruments Inc., Model PC 6011). The temperature gradient between the inside and the outside of the reactor was observed to change from 10 to 50 K depending upon the reactor temperature. All the temperatures reported in the experiments were gas-phase temperatures measured inside the reactor.

Materials

The silica-supported Pt catalysts were prepared from solutions containing the appropriate weight of $H_2PtCl_6 \cdot 6H_2O$ (Strem Chemical). The solution was added to a predetermined weight of Cab-O-Sil (grade M-5, surface area 200 m^2/g, Cabot Corp., Boston MA), using a rotovapor in a dropwise manner. The concentration of the metal precursors in the solution used for impregnation was adjusted to give a nominal metal loading of 1% by weight of Pt. The resulting catalysts were dried at room temperature under vacuum. For use in the spectroscopic reactor, the sample disks were prepared by pressing the ground catalysts (50 to 80 mesh) into self-supporting disks 1.25 cm in diameter with an optical density of approximately 80 mg/cm^2.

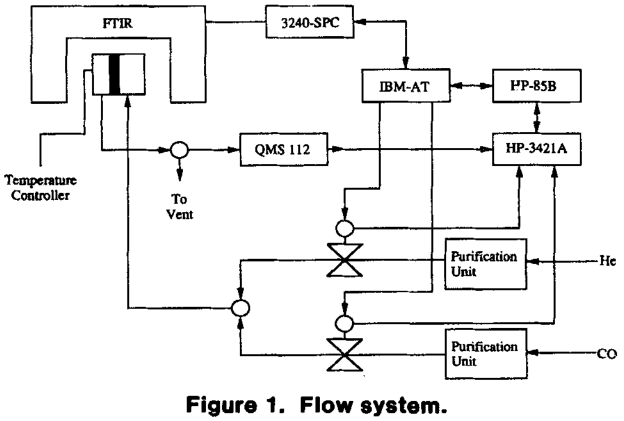

Figure 1. Flow system.

The total flow rate was kept constant at 100 mL/min. The steady-state concentration of CO in the feed gas was 2% and was generally varied by no more than 1% during the sinusoidal perturbations. All the gases used were research grade or better and were purchased from the Linox Co., Chicago, Illinois. The concentration of O_2 in the He carrier gas was reduced to less than 0.2 ppm through the use of a molecular sieve maintained at 200 K, an oxygen purifier (Supelco Co.) and an MnO trap activated in H_2 at 673 K.

Chemisorption measurements were performed by using the dynamic pulse method (Sarkany and Gonzalez, 1982). Metal dispersions were calculated on the basis of a CO/Pt adsorption stoichiometry of 0.89 (Sarkany and Gonzalez, 1983). These adsorption ratios had been established moderately well and resulted in a Pt dispersion of 22.4%.

Procedure

Prior to a transient study, the freshly pressed sample disks were reduced according to the following schedule:

- The catalyst was exposed to flowing He (100 mL/min) at 323 K.
- The temperature was then increased at a linear rate of 10 K/min to 423 K in flowing He and maintained at 423 K for 0.5 h.
- The He flow was switched to H_2 (100 mL/min) at 150°C and the temperature was then increased at 10 K/min to 728 K.
- The catalyst was reduced in flowing H_2 for 3 h at 728 K followed by treatment in flowing He for 0.5 h at the same temperature.
- The temperature was then reduced to 323 K in flowing He.

Two different temperatures, 343 K and 429 K, were chosen to perform the phase lag studies. Following the initial unstable transient period, the phase lag between the inlet gaseous CO and CO adsorbed on the surface was measured during the steady-state response period. The surface coverage of CO was obtained from the ratio of the absorbance of CO to that obtained at saturation surface coverage. This assumes a linear CO absorption extinction coefficient over the small range of surface coverage changes induced by the perturbation. This assumption is reasonably well documented (Eischens and Pliskin, 1958).

Results

The results of a representative phase lag study are shown in Figure 2. In this figure, the infrared absorbance of the CO stretching frequency centered at 2,080 cm^{-1} is plotted as a function of time for a forcing frequency of 0.3 rad/s. Figure 2a is the initial response of CO coverage to the forcing input function, while figure 2b is the steady-state response which is used for the measurement of the phase lag. The maximum variation in the absorbance was about 0.01 absorbance units. The sinusoidal fluctuations in the gas-phase concentration of CO entering the reactor are superimposed on the fluctuations in the absorbance of CO adsorbed on the surface. The phase lag can easily be extracted from these two curves for this particular choice of forcing frequency.

The plot of the tangent of phase lag vs. forcing frequency is shown in Figure 3. From the phase lag jumps shown in Figure 3,

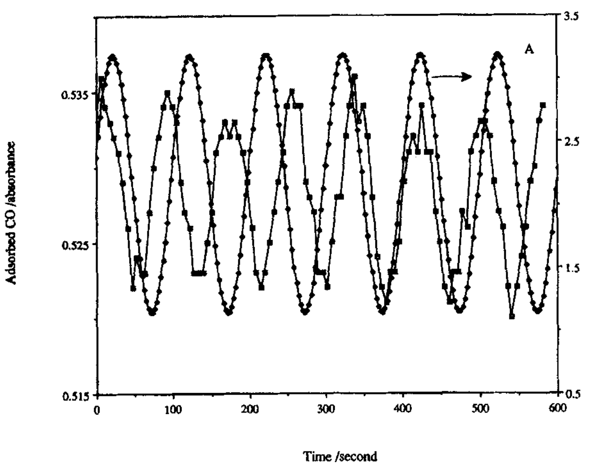

Figure 2a. Typical single experiment data point for the transient response: CO absorbances vs. time.

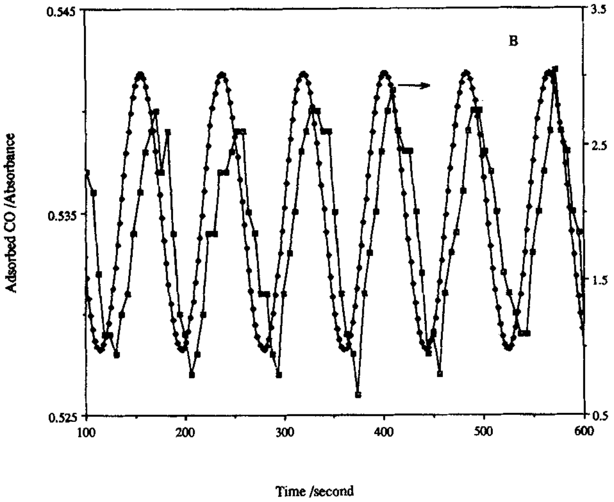

Figure 2b. Typical single experiment data point for the stable response: CO absorbances vs. time.

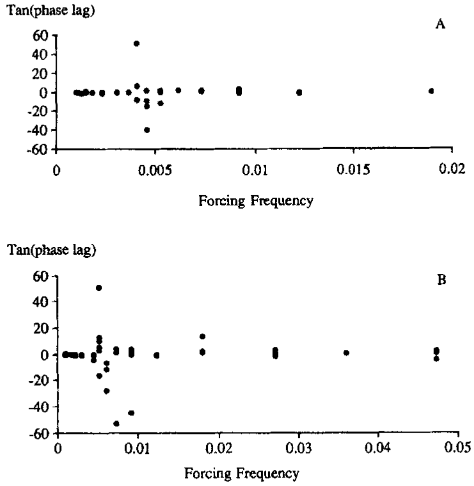

Figure 3. Experimental values of the tangent of the phase lag as a function of forcing frequency.

Flow rate = 100 mL/min; steady-state concentration of CO = 3% in He.

(A) $T = 429$ K and (B) $T = 343$ K.

the critical frequencies of 0.0068 ± 0.0006 at 343 K and 0.0054 ± 0.0008 at 429 K were obtained. At these particular critical forcing frequencies, the gains (i.e., the amplitude ratio of the response function divided by the forcing function) at 70 and 429 K were determined to be 0.0266 and 0.0049, respectively. From the critical forcing frequency and gain, adsorption rate constants at 343 K and 429 K were calculated to be 0.147 s^{-1} and 0.383 s^{-1}, respectively. These adsorption rate constants are about an order of magnitude lower than those experimentally determined by Ertl et al. (1982) for the adsorption of CO on Pt(100).

The desorption rate constant, K_d, can in principle be determined from a knowledge of the residence time (τ), the total number of Pt surface sites exposed (L), and the experimentally determined adsorption rate constant (K_a) through the use of Eq. 8. Because the desorption rate constant, K_d, is approximately three orders of magnitude less than K_a at 343 K, however, it is very difficult to calculate it from the experimentally measured value of Y (Eq. 8). Because the desorption of CO from Pt is activated, there should be a temperature for which the adsorption and desorption rate constants can be deconvoluted from the data and calculated for a given value of Y. Using an activation energy of 193 kJ/mol · deg and a preexponential factor of 10^{13} s^{-1}, this temperature is calculated to be about 1,373 K. Unfortunately, the nature and design of the infrared-cell reactor does not allow us to perform an experiment at this temperature. At low temperatures, however, the problem can be circumvented, provided that the equilibrium constant for adsorption and desorption is available. An equilibrium constant can be obtained from a Langmuir plot, i.e., a plot of $1/\theta$ vs. $1/p$, provided that a linear plot is obtained. Using this approach a desorption rate constant of 7.28×10^{-3} s^{-1} was obtained at 343 K. This value is considerably larger than the value of 6.5×10^{-7} s^{-1} obtained by Herz et al. (1982) using temperature programmed desorption from an aluminum oxide supported Pt catalyst.

A knowledge of the rate constants for adsorption enables one to calculate the sticking coefficients through the use of the equation:

$$r_a = s\frac{P/N_a}{\sqrt{2\pi m_a k_B T}} \qquad (15)$$

where s is the sticking coefficient, and the second term in the equation represents the collision frequency obtained from simple gas-phase kinetic theory. The results of this study are summarized in Table 1.

Discussion

A method based upon transmission FTIR has been developed which enables the measurement of adsorption and desorption rate constants. Due to temperature constraints, however, only the rate constant for adsorption was measured directly. At low temperatures, the rate constant for desorption was obtained from a knowledge of the adsorption-desorption equilibrium constant.

The desorption rate constant obtained at 343 K is considerably larger than that obtained by the temperature programmed

Table 1. Rate Constants Obtained by Frequency Response Technique

Temp. K	Critical Frequency ω_c	Critical Gain M_c	Adsorption Rate Constant K_a, s^{-1}	Sticking Coefficient	θ_∞ %
343	0.0068 ± 0.0006	0.0266	0.147 ± 0.012	0.013 ± 0.001	92
429	0.0054 ± 0.0008	0.0049	0.383 ± 0.027	0.010 ± 0.001	60

desorption method. This is what one would expect. At low temperatures, only molecules which are weakly adsorbed on the surface are perturbed by fluctuations in the forcing input function. The rate constants obtained in this study are the rate constants for the reversible weakly adsorbed CO. Figure 4 shows that the amount of weakly-adsorbed CO corresponds to about 20% of the total CO adsorbed. The maximum absorbance of adsorbed CO shown in Figure 4 levels off at about 1.1 absorbance units. The horizontal arrow shown in Figure 4 corresponds to the experimental concentration fluctuations used in this study. It is also important to note that hysteresis was not observed when the partial pressure of CO was increased and then decreased. This indicates that CO is reversibly adsorbed and desorbed from the surface. Rate constants from the TPD method represents a convoluted average of both strongly and weakly adsorbed CO.

The desorption rate constants at higher temperatures cannot be calculated from the equilibrium constants, because the equilibrium constants at these temperatures are convoluted constants which include both weakly and strongly adsorbed CO. This is immediately apparent from the nonlinearity of the resulting Langmuir plots.

The sticking coefficients determined from this study vary from 10^{-2} at 90% CO coverage and 343 K to 10^{-1} at 60% CO coverage and 429 K. The observed increase in the sticking coefficient by one order of magnitude when the temperature is increased from 70 to 429 K is primarily due to the drop in CO surface coverage from 90 to 60%. The functional relationship between the sticking coefficient and coverage agrees well with published single crystal data. On Pt(111), Ertl et al. (1982) found that the sticking coefficient drops from 0.9 to 0 as the CO coverage is increased from 0% to 50%.

Experimentally, the phase lag of the response represents an additive contribution from adsorption, desorption, and pore diffusion. The theoretical model which we have developed neglects the contribution of pore diffusion. For this reason, it is important to justify the neglect of pore diffusion in the measurement of adsorption and desorption rate constants.

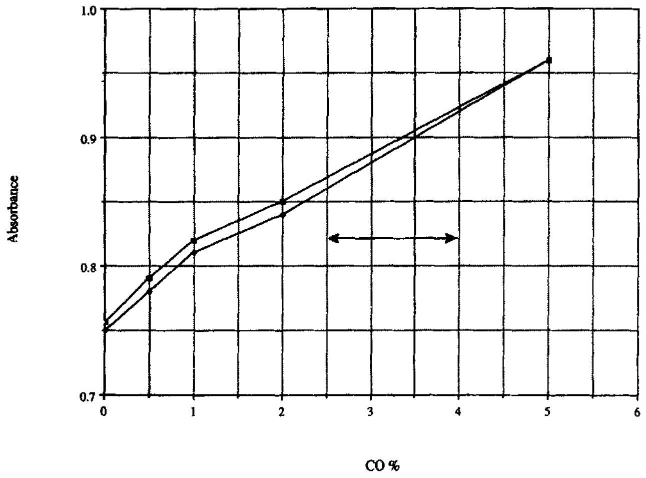

Figure 4. Partial pressure of CO as a function of the absorbance of CO on Pt/SiO$_2$.

If the diffusion process is considered in the absence of adsorption and desorption, the response of the system as a function of the sinusoidal forcing input can be mathematically expressed by Fick's second law. The time lag due to diffusion is therefore:

$$t_{\text{diffusion}} = \sqrt{\frac{1}{2D\omega}}\, z \qquad (16)$$

Because Cab-O-Sil, which has essentially no micropore structure, was used as the support, only bulk diffusion within the macropore structure of the pressed catalyst disk was considered. Use of the Chapman-Enskog equation (Hirschfelder et al., 1954) yields a diffusion coefficient of 6.4 × 10^{-2} cm^2/s. The thickness of the pellet is 0.01 cm. Use of these values together with Eq. 16 results in a time lag due to diffusion of 0.093 and 0.100 s, respectively, for the critical forcing frequencies used. These values are much smaller than the experimentally measured values of 41.7 ± 5.3 and 51.8 ± 1.9 s. Furthermore, if we compare the phase lags calculated from the forcing frequencies

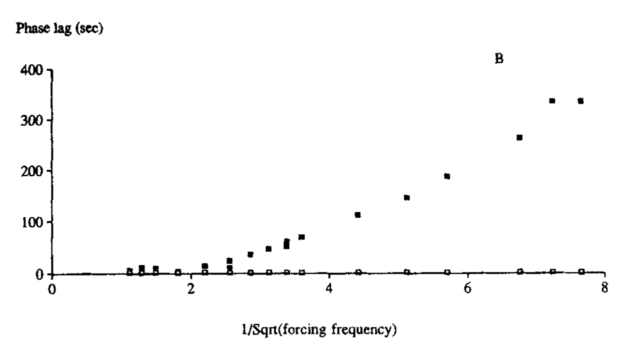

Figure 5. Comparison of the theoretical- and experimental-phase lags as a function of the square root of forcing frequency.

(A) $T = 429$ K and (B) $T = 343$ K.
The theoretical values were calculated using Eq. 16.
■ experimental values; □ theoretical values.

based upon Eq. 16 to the experimental values as is shown in Figure 5, it is clear that the experimental data points do not fall into the predicted line given by Eq. 16. Hence, it is apparent that the neglect of pore diffusion is justified.

Conclusions

The method outlined and tested in this study offers some real advantages over methods currently being used. The rate constants are obtained under "real flow conditions" with no pseudosteady-state assumptions being made. As a disadvantage, the method requires the use of some rather specialized equipment and the measurements require considerable effort. The method can be applied to the adsorption and desorption of reactant molecules regardless of the order of the process, i.e., both associative and dissociative adsorption can be studied. The only requirement is that the adsorbed species should give rise to absorption frequencies which are readily detectable in the infrared.

Acknowledgment

We acknowledge support from the donors of the Petroleum Research Fund, administered by the American Chemical Society, for this research. We also would like to thank Lambert Lucietto of the Byron-Lambert Co., Franklin Park, IL, for his much-needed input in overcoming numerous technical problems associated with the infrared cell reactor; Yao-En Li thanks the University of Illinois for a University Fellowship. Finally, we are grateful to the U.S. Department of Energy (Grant DOE FC02-86ER-13531) for funding the purchase of a large portion of the equipment used in this research.

Notation

k_B = Boltzman constant
m = order of reaction
m_a = molecular weight
n_i = adsorbed species i, mol
n^{in} = inlet species i, mol
n_g = species i in the gas phase, mol
p = partial pressure, atm
s = sticking coefficient
t = real time, s
z = thickness of the catalyst pellet, cm
D = diffusion coefficient, $\mathrm{cm}^2 \cdot \mathrm{s}^{-1}$
F = total volumetric flow rate, $\mathrm{mL} \cdot \mathrm{s}^{-1}$
$G(s) = X/\alpha s^2 + (Y + \alpha + \alpha X)s + Y$
K_a = adsorption rate constant, $\mathrm{s}^{-1} \cdot \mathrm{mol}^{-1} \cdot \mathrm{mL}$
K_d = desorption rate constant, s^{-1}
L = total number of exposed active catalytic sites, mol
N_a = Avogadro's number
T = temperature, K
K = equilibrium constant
$K_1 = K_a \tau L^m$
$K_2 = K_d \alpha \tau L^{-(m-1)}$
M = amplitude ratio of response over input
M_c = critical amplitude ratio of response over input at critical forcing frequency
$N = n_g/n^{ss}$
$N^{in} = n^{in}/n^{ss}$

Greek letters

$\alpha = L/n^{ss}$
ϕ = phase lag
θ = coverage, n_i/L
θ^{ss} = steady state coverage
$\xi = t/\tau$
τ = residence time, =volume of catalyst bed/total flow rate, s
ω = frequency times residence time

Literature Cited

Eischens, R. P., and W. A. Pliskin, "The Infrared Spectra of Adsorbed Molecules," *Adv. Cat.*, **10**, 1 (1958).

Ertl, G., and T. Engel, *The Chemical Physics of Solid Surfaces and Heterogeneous Catalysis*, **4**, 73, D. A. King and J. P. Woodruff, eds., Elsevier, Amsterdam (1982).

Goodwin, Jr., J. G., J. E. Lester, G. Marcelin, and S. F. Mitchell, "Frequency Response Chemisorption Studies of Carbon Monoxide Hydrogenation Catalysts," *ACS Symp. Ser.*, 288(1985).

Hirschfelder, J. O., C. F. Curtiss, and R. B. Bird, "Molecular Theory of Gases and Liquids," 539, 578, Wiley, New York (1954).

Herz, R. K., J. B. Kiela, and S. P. Marin, "Adsorption Effects during Temperature-Programmed Desorption of Carbon Monoxide from Supported Paltinum," *J. Cat.*, **73**, 66 (1982).

Jones, R. H., D. R. Olander, W. J. Siekhaus, and J. A. Schwarz, "Investigation of Gas-Solid Reactions by Modulated Molecular Beam Mass Spectrometry," *J. Vac. Sci. Technol.*, **9**(6), 1429 (1972).

Nagai, M., L. L. Lucietto, Yao-En Li, and R. D. Gonzalez, "An Improved Infrared Cell Reactor for Use in Transient Response Studies: The Catalytic Oxidation of CO Reexamined," *J. Cat.*, **101**, 522 (1986).

Naphtali, L. M., and L. M. Polinski, "A Novel Technique For Characterization of Adsorption Rates on Heterogeneous Surfaces," *J. Phys. Chem.*, **67**, 369 (1963).

Sarkany, J., and R. D. Gonzalez, "The Measurement of Extinction Coefficients Using A New Infrared Micropulse Reactor Technique: Adsorption Of CO On Silica Supported Pt," *J. Appl. Spectrosc.*, **36**, 320 (1983a).

———, "On the Use of the Dynamic Pulse Method to Measure Metal Surface Areas," *J. Cat.*, **76**, 75 (1982).

———, "Support and Dispersion Effects on Silica and Alumina Supported Pt Catalysts," *J. Appl. Cat.*, **4**, 53 (1983b).

Schwarz, J. A., and R. J. Madix, "Modulated Beam Relaxation Spectrometry: Its Application to the Study of Heterogeneous Kinetics," *Surf. Sci.*, **46**, 317 (1974).

Yasuda, Y. "Frequency Response Method for Study of the Kinetic Behavior of a Gas-Surface System: 1. Theoretical Treatment," *J. Phys. Chem.*, **80**(17), 1867 (1976).

Manuscript received Mar. 28, 1988, and revision received Dec. 9, 1988.